CHROM. 21 306

NEW METHOD FOR MEASURING OBSTRUCTIVE FACTORS AND POROSITY USING GAS CHROMATOGRAPHIC INSTRUMENTATION

N. A. KATSANOS* and Ch. VASSILAKOS

Physical Chemistry Laboratory, University of Patras, 26110 Patras (Greece)

SUMMARY

A method for measuring obstructive factors γ and the external porosity ε in solid beds by using the reversed-flow gas chromatographic technique is described. The method does not have any of the disadvantages connected with the carrier gas flow and the instrumental spreading of the chromatographic bands, because the phenomena being studied are taking place inside a diffusion column through which no carrier gas flows. Measurements of elution velocities, height equivalent to a theoretical plate and theoretical diffusion coefficients are not needed, the calculations being based simply on the slopes of three linear plots obtained experimentally. The necessary mathematical equations are derived in detail and applied to determine the γ and ε values with six packing materials, using four different glass cells.

INTRODUCTION

A flow perturbation technique, reversed-flow gas chromatography (RF-GC), was introduced in 1980[1] and used to study the kinetics of various surface-catalysed reactions[2–12] and for other physico-chemical measurements. The latter include gas diffusion coefficients[13–15], relative molar responses, collision diameters and critical volumes of gases[16], Lennard–Jones parameters[17], adsorption equilibrium constants[18], the kinetics of drying of catalysts[19], rate coefficients for evaporation of pure liquids[20], activity coefficients in liquid mixtures[21], kinetic studies of reactivity of marble with sulphur dioxide[22], interaction between the components of salt-modified adsorbents[23] and mass transfer and partition coefficients across phase boundaries[24–27]. Two general reviews on the method have have published[28,29], a review on the analytical applications of the method[30] and recently a book[31].

The new technique is based on reversing the direction of flow of the carrier gas from time to time. It uses a conventional gas chromatograph with any kind of detector, accommodating in its oven a so-called sampling cell. This consists of a sampling column and a diffusion column and is connected to the carrier gas inlet and the detector via a four- or six-port valve, as shown schematically in Fig. 1. By switching the valve from one position to the other, the carrier gas is made to flow through the sampling column either from D_2 to D_1 or in the reverse direction. It also fills the
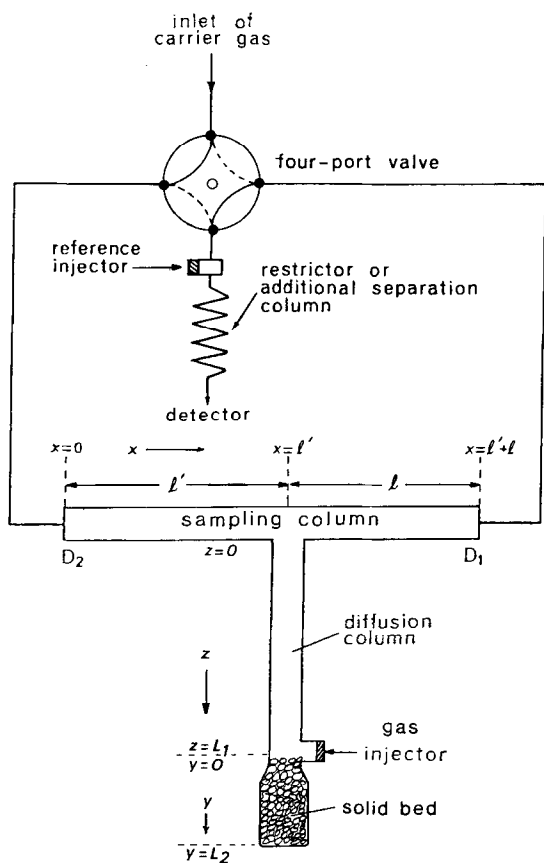
Fig. 1. Gas connections and columns in the RF-GC technique (from ref. 30).

diffusion column L_1 and the vessel L_2. More details of the experimental set-up used with the RF-GC technique can be found elsewhere[29,31].

The flow reversal for a time period t' shorter than the gas hold-up time of a solute in the sections l and l' of the sampling column records the concentration of the solute in the junction $x = l'$, if this solute comes out of column L_1 as the result of its diffusion into the carrier gas. This concentration recording has the form of extra chromatographic peaks (sample peaks) superimposed on the otherwise continuous detector signal. An example is given in Fig. 2. The area under the curve or the height h from the continuous concentration–time curve of these sample peaks, measured as a function of time t_0 (when the flow reversal was made) is the basic mathematical tool giving the physico-chemical quantities mentioned above.

In most instances this is done in a simple, although accurate way, using cheap conventional GC instrumentation, without the need to perform any of the usual gas chromatographic operations and measurements. An example is provided by the accurate measurement of gaseous diffusion coefficients[13-15], without concern for the main difficulties associated with the traditional GC methods, e.g., the disadvantages
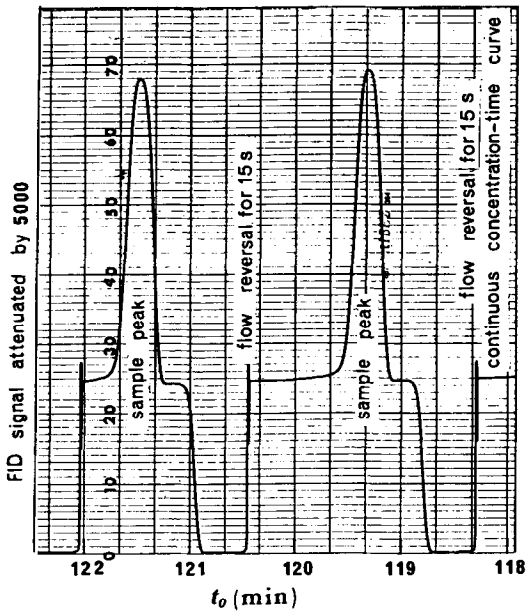
Fig. 2. A reversed-flow chromatogram with two sample peaks recording the concentration of propene in nitrogen at $x = l'$ ($\dot{V} = 0.36$ cm^{3}s^{-1}, $T = 324.7$ K, $p = 1$ atm) (from ref. 26).

inherent in operation at low flow-rates and the difficulty of correctly allowing for the instrumental spreading of the chromatographic band outside the column. The same and other problems are met in the determination of the obstructive factor γ, as it is the product γD which is usually determined from HETP measurements in packed columns, employing a range of carrier gas velocities around the optimum value. Then, γ is usually found by assuming a theoretical value for the diffusion coefficient D. An additional disadvantage of this method is that the experimental data are fitted to an height equivalent to a theoretical plate (HETP) equation, assumed to be correct.

The arrested elution method of Knox and McLaren[32] bypasses some of the experimental and theoretical difficulties of the standard continuous elution method, but it still relies heavily on the time of passage along the column and the accurate measurement of the outlet elution velocity.

The RF-GC technique does not have any of the disadvantages connected with the carrier gas flow and the instrumental spreading of the chromatographic bands, because the phenomena being studied are taking place inside the diffusion column L_1 and the vessel L_2, and no carrier gas flows through those vessels. The gas flows only through the column $l' + l$, and is merely used as a means for repeated sampling of the concentrations at the point $x = l'$, i.e., at the exit of the column L_1. This is done with the help of the narrow and symmetrical sample peaks, mentioned above (cf., Fig. 2), without measuring their elution velocity and without even knowing the carrier gas flow-rate. The experimental data recorded are the height h of the sample peaks in arbitrary units (say cm), and the time t_0 elapsing between the solute injection and the respective flow reversal, the duration of the latter being always the same (say 30 s). If
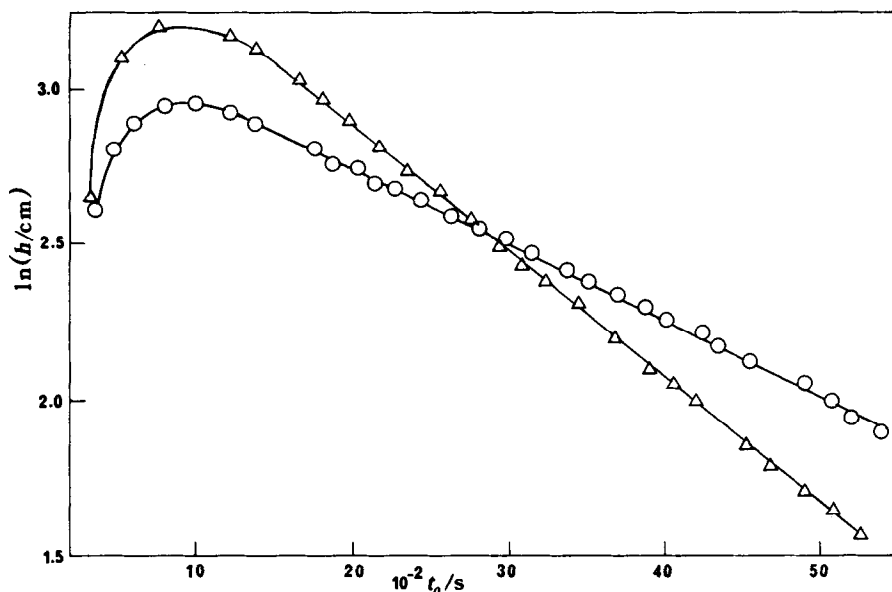
Fig. 3. Diffusion bands obtained at 313.2 K with a thermal conductivity detector, using helium as carrier gas and nitrogen as solute. $\bigcirc$, Vessel L_2 empty; $\triangle$, vessel L_2 filled with glass beads of diameter 3 mm.

one plots $\ln h$ against t_0, a so-called diffusion band is obtained, like those shown in Fig. 3.

An obvious difference between the old elution GC and RF-GC is that in the former longitudinal gaseous diffusion currents are parallel to the chromatographic current and the diffusion coefficients D or γD are extracted from this mixed current by mathematical analysis. In the second method, the diffusion current is from the outset physically separated from the chromatographic current, and this is done by placing the diffusion process perpendicular to the chromatographic process. A diffusion band, rather than an elution band, is now mathematically analysed to yield diffusion coefficients, or other physico-chemical parameters from its distortion, in the same way that a distorted elution chromatographic band permits similar calculations. It must be pointed out that instrumental or other spreading of the sample peaks does not influence the results, as it is the same in all peaks of the same run. If the duration of the flow reversals is changed, the above spreading changes, but the physico-chemical quantity extracted from the diffusion band comes out the same, provided that the same duration is maintained in all flow reversals in the same experiment.

A general chromatographic sampling equation, describing the concentration–time curve of the sample peaks created by the flow reversals, has been derived[14,28,31] using mass balances, rates of change, etc., and integrating the resulting partial differential equations under given initial and boundary conditions. It was proved[28,31], however, that the height h of each sample peak above the ending baseline is proportional to the concentration of the solute at the junction $x = l'$ of the sampling cell and at time t_0 of the flow reversal. This peak height for a linear detector, like the flame ionization detector, is given by the relation

$$h \approx 2c(l', t_0) \tag{1}$$

MATHEMATICAL ANALYSIS

The function for the diffusion band

The mathematical function describing the diffusion band has been derived for some specific cases, namely, (a) when no vessel L_2 exists[31] and the diffusion column is empty and closed at $z = L_1$ (*cf.*, Fig. 1); (b) when L_2 is absent and column L_1 is filled with a reactive solid[22]; (c) when vessel L_2 contains an agitated liquid[26]; (d) when vessel L_2 is filled with a reactive solid[27,30]. In all these derivations, various degrees of approximations were adopted in solving the differential equations, according to the precision required and the complexity of the problem. In the present case the function for the diffusion band is sought independently of the gas injected into the cell, with a better precision than before, and for the following arrangements: (1) when both column L_1 and vessel L_2 are empty of any solid or liquid material; (2) when both column L_1 and vessel L_2 are packed with a solid material that does not interact in any way with the injected solute; and (3) when L_1 is empty and only L_2 is packed with the above solid. Case 3 gives a general solution with 1 and 2 as special cases. Therefore, it is treated first.

Following the same mathematical practice as before[22,26,27,29,31], the diffusion equation (Fick's second law) is written for the regions z and y (*cf.*, Fig. 1):

$$\partial c_z / \partial t_0 = D_1 \partial^2 c_z / \partial z^2 \tag{2}$$

$$\partial c_y / \partial t_0 = D_2 \partial^2 c_y / \partial y^2 \tag{3}$$

where $c_z = c_z(z, t_0)$ and $c_y = c_y(y, t_0)$ are the gaseous concentrations of the injected solute in the region z (diffusion column) and y (vessel L_2), respectively, D_1 and D_2 being the gaseous diffusion coefficients of the solute in the carrier gas in regions z and y, respectively.

The initial conditions are

$$c_z(z, 0) = \frac{m}{a_G} \delta(z - L_1) \tag{4}$$

$$c_y(y, 0) = 0 \tag{5}$$

where m is the amount of solute injected at $z = L_1$, a_G the cross-sectional area in column z (and also in column $l' + l$) and $\delta(z - L_1)$ the Dirac delta function.

There are boundary conditions at three regions: at $z = 0$, at $z = L_1$ or $y = 0$, and at $y = L_2$:

$$c_z(0, t_0) = c(l', t_0) \tag{6}$$

$$D_1 (\partial c_z / \partial z)_{z=0} = vc(l', t_0) \tag{7}$$

$$c_z(L_1, t_0) = c_y(0, t_0) \tag{8}$$

$$a_G D_1 (\partial c_z / \partial z)_{z=L_1} = a'_G D_2 (\partial c_y / \partial y)_{y=0} \tag{9}$$

$$(\partial c_y / \partial y)_{y=L_2} = 0 \tag{10}$$

where $c(l', t_0)$ is the solute concentration at $x = l'$ given in eqn. 1, v is the linear velocity of the carrier gas and a'_G the cross-sectional area of vessel L_2.

The system of partial differential equations 2 and 3 can be solved by using Laplace transformation with respect to t_0 (transform parameter p_0), under the initial conditions 4 and 5, and subject to the boundary conditions 6–10. The first results are two ordinary linear second-order differential equations in $C_z(z, p_0)$ and $C_y(y, p_0)$, the capital letters C_z C_y denoting the t_0 Laplace transformed functions c_z and c_y, respectively:

$$\frac{d^2C_z}{dz^2} - q_1^2 C_z = -\frac{m}{a_G D_1}\delta(z - L_1) \tag{11}$$

$$\frac{d^2C_y}{dy^2} - q_2^2 C_y = 0 \tag{12}$$

where

$$q_1^2 = p_0/D_1 \quad \text{and} \quad q_2^2 = p_0/D_2 \tag{13}$$

Both eqns. 11 and 12 can be integrated either classically or by using z and y Laplace transformation, respectively, with the following results:

$$C_z = C_z(0)\cosh q_1 z + \frac{C'_z(0)}{q_1} \sinh q_1 z - \frac{m}{a_G D_1 q_1} \sinh q_1(z - L_1) \cdot u(z - L_1) \tag{14}$$

$$C_y = C_y(0)\cosh q_2 y + \frac{C'_y(0)}{q_2} \sinh q_2 y \tag{15}$$

where $C_z(0)$ and $C_y(0)$ are the t_0 transforms of c_z and c_y at $z = 0$ and $y = 0$, respectively, $C'_z(0) = (dC_z/dz)_{z=0}$, $C'_y(0) = (dC_y/dy)_{y=0}$ and $u(z - L_1)$ is the Heaviside unit step function, with values 0 for $z < L_1$ and 1 for $z \geqslant L_1$.

The values or the relations of $C_z(0)$, $C'_z(0)$, $C_y(0)$ and $C'_y(0)$, which would be constants of integration had eqns. 11 and 12 been solved classically, can be found with the help of the boundary conditions 6–10, all transformed with respect to t_0, thereby changing c_z, c_y and c to C_z, C_y and C, respectively. Therefore, $C_z(0)$ is replaced by $C(l', p_0)$ according to eqn. 6, and $C'_z(0)$ is substituted by $vC(l', p_0)/D_1$ from eqn. 7, giving

$$C_z = C(l', p_0)(\cosh q_1 z + \frac{v}{D_1 q_1} \sinh q_1 z) - \frac{m}{a_G D_1 q_1} \sinh q_1(z - L_1) \cdot u(z - L_1) \tag{16}$$

whereas, by using eqn. 10, eqn. 15 is simplified to

$$C'_y(0) = -C_y(0)q_2\tanh q_2 L_2 \tag{17}$$

Finally, eqns. 16 and 17 are linked together using the boundary conditions 8 and 9, with the result

$$C(l', p_0) = \frac{m}{a_G D_1 q_1}[\sinh q_1 L_1 + \frac{v}{D_1 q_1}\cosh q_1 L_1 + \frac{a'_G D_2 q_2}{a_G D_1 q_1}\tanh q_2 L_2(\cosh q_1 L_1 +$$

$$+ \frac{v}{D_1 q_1}\sinh q_1 L_1)]^{-1} \tag{18}$$

This relationship is similar to eqn. 21 in ref. 27, but some of the approximations used to effect its inverse Laplace transformation with respect to p_0 are now different, leading to a more precise result. First, it is assumed as before that $v/D_1 q_1 \gg 1$ for high enough flow velocities and $\sinh q_1 L_1$ is omitted compared with $(v/D_1 q_1)\cosh q_1 L_1$, and also $\cosh q_1 L_1$ compared with $(v/D_1 q_1)\sinh q_1 L_1$. After this approximation, and some rearrangement, eqn. 18 becomes

$$C(l', p_0) = \frac{m}{\dot{V}}\left[D_1 q_1 \sinh q_1 L_1\left(\frac{\coth q_1 L_1}{D_1 q_1} + \frac{a'_G D_2^2 q_2^2}{a_G D_1^2 q_1^2}\cdot\frac{\tanh q_2 L_2}{D_2 q_2}\right)\right]^{-1} \tag{19}$$

where $\dot{V} = a_G v$ is the volume flow-rate of the carrier gas.

The following approximations are new and adopted for the first time. These refer to the hyperbolic functions $\sinh q_1 L_1$, $\coth q_1 L_1$ and $\tanh q_2 L_2$. The first is simply set equal to the argument $q_1 L_1$, but the latter two functions are subject to the following procedure. First, the inverse Laplace transforms of $\coth q_1 L_1/D_1 q_1$ and $\tanh q_2 L_2/\dot{D}_2 q_2$ are taken[33] in the form of an elliptic function θ_3 or θ_2, respectively, and then the series representing each θ function is transformed back, term by term, to obtain

$$\frac{\coth q_1 L_1}{D_1 q_1} = \frac{1}{L_1}\left(\frac{1}{p_0} + \frac{2}{p_0 + \beta} + \frac{2}{p_0 + 4\beta} + \frac{2}{p_0 + 9\beta} + \cdots\right) \tag{20}$$

$$\frac{\tanh q_2 L_2}{D_2 q_2} = \frac{2}{L_2}\left(\frac{1}{p_0 + \alpha} + \frac{1}{p_0 + 9\alpha} + \frac{1}{p_0 + 25\alpha} + \cdots\right) \tag{21}$$

where

$$\beta = \pi^2 D_1/L_1^2 \tag{22}$$

$$\alpha = \pi^2 D_2/4L_2^2 \tag{23}$$

The approximation starts from this point by omitting the time parameter p_0 from a particular term onwards as compared with the diffusion parameters $n\beta$ or $n\alpha$. In series 20, p_0 is omitted compared with 4β, 9β, ..., etc., while in series 21, p_0 is omitted in comparison with 9α, 25α, ..., etc.:

$$\frac{\coth q_1 L_1}{D_1 q_1} \approx \frac{1}{L_1}\left[\frac{1}{p_0} + \frac{2}{p_0 + \beta} + \frac{2}{\beta}\left(\frac{1}{4} + \frac{1}{9} + \frac{1}{16} + \cdots\right)\right]$$

$$= \frac{1}{L_1}\left(\frac{1}{p_0} + \frac{2}{p_0 + \beta} + \frac{2}{\beta} \sum_{n=1}^{\infty} \frac{1}{n^2} - \frac{2}{\beta} \right)$$

$$= \frac{1}{L_1}\left(\frac{1}{p_0} + \frac{2}{p_0 + \beta} + \frac{2}{\beta} \cdot \frac{\pi^2}{6} - \frac{2}{\beta} \right)$$

$$= \frac{1}{L_1}\left(\frac{1}{p_0} + \frac{2}{p_0 + \beta} + \frac{1.29}{\beta} \right) \tag{24}$$

$$\frac{\tanh q_2 L_2}{D_2 q_2} \approx \frac{2}{L_2}\left[\frac{1}{p_0 + \alpha} + \frac{1}{\alpha}\left(\frac{1}{9} + \frac{1}{25} + \ldots \right) \right]$$

$$= \frac{2}{L_2}\left[\frac{1}{p_0 + \alpha} + \frac{1}{\alpha} \sum_{n=0}^{\infty} \frac{1}{(2n + 1)^2} - \frac{1}{\alpha} \right]$$

$$= \frac{2}{L_2}\left(\frac{1}{p_0 + \alpha} + \frac{1}{\alpha} \cdot \frac{\pi^2}{8} - \frac{1}{\alpha} \right) \tag{25}$$

The sums $\sum_{n=1}^{\infty} n^{-2}$ and $\sum_{n=0}^{\infty} (2n + 1)^{-2}$ are evaluated as equal to $\pi^2/6$ and $\pi^2/8$, respectively, by means of the Riemann zeta function.

Approximating in eqn. 19 the function $\sinh q_1 L_1$ by $q_1 L_1$, $(\coth q_1 L_1)/D_1 q_1$ by the far right-hand side of eqn. 24 and $(\tanh q_2 L_2)/D_2 q_2$ by the far right-hand side of eqn. 25, one obtains, after rearrangement, an equation containing only numerical constants and three dimensionless parameters λ, A and R:

$$C(l', p_0) = \frac{m}{\dot{V}}(A\lambda + 1)(\lambda + 1)[A(1.29 + 1.87R)\lambda^3 +$$

$$+ (1.29 + 4.29A + \pi^2 R + 1.87AR)\lambda^2 + (4.29 + A + \pi^2 R)\lambda + 1]^{-1} \tag{26}$$

where

$$\lambda = p_0/\beta \tag{27}$$

$$A = \frac{\beta}{\alpha} = \frac{4L_2^2}{L_1^2} \cdot \frac{D_1}{D_2} \tag{28}$$

$$R = \frac{a_G' L_2}{a_G L_1} = \frac{V_G'}{V_G} \tag{29}$$

$V_G = a_G L_1$ and $V_G' = a_G' L_2$ being the gaseous volumes of column L_1 and vessel L_2, respectively. If the roots of the denominator in eqn. 26 are $-r_1$, $-r_2$ and $-r_3$, this equation is simply written as

$$C(l', p_0) = \frac{m}{VA(1.29 + 1.87R)} \cdot \frac{(A\lambda + 1)(\lambda + 1)}{(\lambda + r_1)(\lambda + r_2)(\lambda + r_3)} \tag{30}$$

and its inverse Laplace transformation with respect to p_0 is easily taken after breaking it into three partial fractions. The result is the desired function $c(l', t_0)$ given as sum of three exponential functions of time:

$$c(l', t_0) = N_1\left[\frac{(Ar_1-1)(r_1-1)}{(r_1-r_2)(r_1-r_3)} \exp(-r_1\beta t_0) + \frac{(Ar_2-1)(r_2-1)}{(r_2-r_1)(r_2-r_3)} \exp(-r_2\beta t_0) + \right.$$

$$\left. + \frac{(Ar_3-1)(r_3-1)}{(r_3-r_1)(r_3-r_2)} \exp(-r_3\beta t_0)\right] \tag{31}$$

where

$$N_1 = \frac{m\beta}{VA(1.29 + 1.87R)} \tag{32}$$

If the right-hand side of eqn. 31 is substituted for $c(l', t_0)$ in eqn. 1, the height h of the sample peaks as a function of time is obtained, *i.e.*, the function describing the diffusion band (*cf.*, Fig. 3), when the column L_1 is empty and the vessel L_2 is packed with a solid not interacting with the injected solute. The ratio D_1/D_2 in this case is equal to $D_1/\gamma D_1 = 1/\gamma$, where γ is the obstructive factor in the packed vessel L_2 as defined by Giddings[34], and also stressed by Knox and McLaren[32] as arising from two effects, namely, the tortuosity of the paths through the medium and the alternating constriction and widening of the paths. Hence the parameter A is given, according to eqn. 28, by

(33) $A = 4L_2^2/L_1^2\gamma$

Eqn. 31 also describes the diffusion band when column L_1 and vessel L_2 are both empty of any solid material or both packed with non-sorbing material. In these two cases, however, $D_1/D_2 = 1$ and

$$A = 4L_2^2/L_1^2 \tag{34}$$

Moreover, the parameter R will have the same value irrespective whether L_1 and L_2 are both empty or packed with solid. Therefore, the values of A and R in these cases are characteristic of the cell dimensions, and with their help the roots $-r_1$, $-r_2$ and $-r_3$ of the denominator in eqn. 26 can be found with any desired precision. These roots differ considerably from one another, making the exponential coefficients $-r_1\beta$, $-r_2\beta$ and $-r_3\beta$ of the three functions in eqn. 31 very different, and therefore easily determinable from the experimental diffusion band. For example, the absolutely smallest root, say $-r_3$, describes the diffusion band at long enough times, *i.e.*, after its maximum (*cf.*, Fig. 3), when the other two exponential functions have already decayed to negligibly low values. It corresponds to the last linear part of the band, as the latter is

a semilogarithmic plot. The slope of this part gives $-r_3\beta$ and , using eqn. 22, the diffusion coefficient D_1 of the solute in the carrier gas is easily calculated.

Two limiting cases of eqn. 31 are worth mentioning. The first arises when $L_2 = 0$ and $V'_G = 0$, i.e., when vessel L_2 is absent. Then, $A = 0$ and $R = 0$, the denominator of eqn. 26 reduces to $1.29\lambda^2 + 4.29\lambda + 1$, with roots $-r_1 = -3.073$ and $-r_2 = -0.2522$, and eqn. 30 becomes

$$C(l', p_0) = \frac{m}{V \cdot 1.29} \cdot \frac{\lambda + 1}{(\lambda + 3.073)(\lambda + 0.2522)}$$

giving on inversion the first limiting case of eqn. 31:

$$c(l', t_0) = \frac{m\beta}{V}[0.2055 \exp(-0.2522\beta t_0) + 0.5697 \exp(-3.073\beta t_0)] \qquad (35)$$

Therefore, the slope of the last linear part is $-0.2522\beta = -0.2522\pi^2 D_1/L_1^2 = -\pi^2 D_1/3.97L_1^2$, which coincides with that predicted by eqn. 4–39 in ref. 31. The second limiting case of eqn. 31 is obtained when $L_2 \ll L_1$ and thus A can be set equal to zero. In that case only the volume ratio $R = V'_G/V_G$ determines the roots of the denominator of eqn. 26, which reduces to

$$C(l', p_0) = \frac{m}{V} \cdot \frac{\lambda + 1}{(1.29 + \pi^2 R)\lambda^2 + (4.29 + \pi^2 R)\lambda + 1} \qquad (36)$$

If these roots are $-r_1$ and $-r_2$, the inverse transform gives, instead of eqn. 31, the expression

$$c(l', t_0) = N'_1\left[\frac{r_1 - 1}{r_1 - r_2} \cdot \exp(-r_1\beta t_0) + \frac{r_2 - 1}{r_2 - r_1} \cdot \exp(-r_2\beta t_0)\right] \qquad (37)$$

where

$$N'_1 = \frac{m\beta}{V(1.29 + \pi^2 R)} \qquad (38)$$

Determination of the obstructive factor, γ

Two experimental plots at the same temperature, using the same cell, are required for this determination: (1) a diffusion band (cf., Fig. 3) with both the diffusion column L_1 and the vessel L_2 empty of any solid material; and (2) a diffusion band with both L_1 and L_2 packed with the solid material under study, provided that a gaseous solute, that is not sorbed by the solid or does not interact with it in any way, is used in the diffusion experiment. If the slopes of the last linear parts after the maximum of the above bands are b(empty) and b(packed), their ratio gives directly the value of the obstructive factor, without any other measurement or correction:

$$\frac{b(\text{packed})}{b(\text{empty})} = \frac{-r_3\beta(\text{packed})}{-r_3\beta(\text{empty})} = \frac{\pi^2\gamma D_1/L_1^2}{\pi^2 D_1/L_1^2} = \gamma \qquad (39)$$

This relationship is based on the fact that the parameters A and R have the same value, given by eqns. 34 and 29, respectively, in both experiments (1) and (2) described above. Therefore, all roots $-r_1$, $-r_2$ and $-r_3$ of eqn. 31 are the same whether the cell is empty or packed. The root $-r_3$ is taken as having the smallest value, thus describing the last linear part of the diffusion band. The value of the diffusion parameter β is given by eqn. 22, with the diffusion coefficient being D_1 when the cell is empty and γD_1 when it is packed with solid.

It must be noted that the simpler functions described by eqns. 37 and 35 lead to exactly the same eqn. 39 with $-r_2$ or -0.2522, respectively, substituted for $-r_3$. This means that the experiments could be conducted with column L_1 alone, without the presence of vessel L_2, although in this instance only the obstructive factor, and not the porosity of the solid bed, could be determined, as is shown below.

Determination of the external porosity, ε

One more diffusion band, in addition to those described under (1) and (2) above, is required for this determination: (3) a band obtained with the diffusion column L_1 empty and vessel L_2 packed with the solid under study. This is case 3 mentioned at the beginning of the Mathematical Analysis section, as leading to the most general solution, i.e., eqn. 31 with A given by eqn. 33. Experimentally, the slope of the last linear part of the band, b(semi-packed), is again required, together with the lengths L_1 and L_2, and the gaseous volumes V_G and V'_G of the empty cell. From these lengths and volumes, the values of A(empty) and R(empty) for the empty cell are calculated using eqn. 34 and 29, respectively. The roots of the denominator (in brackets) of eqn. 26 are then found by using the above values of A(empty) and R(empty), as all the others are known numerical constants. The absolutely smallest root, $-r_3$, multiplied by $\beta = \pi^2 D_1/L_1^2$, gives the slope of the last linear part of the band obtained in experiment 1:

$$b(\text{empty}) = -r_3\pi^2 D_1/L_1^2 \tag{40}$$

From this relation, D_1 is accurately calculated, although its value is not required for the present purposes.

The root $-r_{3s}$ for case 3, i.e., for the semi-packed cell cannot be found in the same way as described above, as now the value of A is calculated using eqn. 33, but the value of R(semi-packed) is not known because V'_G(packed) for the packed vessel L_2 is unknown and equal to εV_G(empty), where ε is the external porosity of the packed solid bed, i.e., its void fraction. Conversely, R(semi-packed) is found using the root $-r_{3s}$, and from that the porosity ε. This is accomplished by calculating the unknown root from the experimental slopes and the known $-r_3$:

$$\frac{b(\text{semi-packed})}{b(\text{empty})} = \frac{-r_{3s}\beta}{-r_3\beta} = \frac{-r_{3s}}{-r_3} \tag{41}$$

where β cancels out, because it has the same value for the empty and the semi-packed cell, pertaining only to L_1 but not to L_2 (cf., eqn. 22). The value of $-r_{3s}$ found by means of eqn. 41 is now substituted for λ in the denominator of eqn. 26, together with A(semi-packed) found by eqn. 33, thus yielding an equation in R(semi-packed), from which its value is calculated:

$$R(\text{semi-packed}) = \frac{1.29Ar_{3s}^3 - (1.29 + 4.29A)r_{3s}^2 + (4.29 + A)r_{3s} - 1}{-1.87Ar_{3s}^3 + (\pi^2 + 1.87A)r_{3s}^2 - \pi^2 r_{3s}} \qquad (42)$$

Finally, the porosity ε is calculated from the ratio

$$\varepsilon = \frac{R(\text{semi-packed})}{R(\text{empty})} = \frac{V_G'(\text{packed})}{V_G'(\text{empty})} \qquad (43)$$

Instead of using the denominator of eqn. 26 for the above calculations, the less precise but simpler eqn. 36 can be employed. Using the known value of $R(\text{empty})$, the two roots of the denominator can be found, and the absolutely smaller of them, $-r_2$, can be used in eqn. 40 to find D_1 (if required) or in eqn. 41 in place of $-r_3$ to find $-r_{3s}$. This is substituted back for λ in the denominator of eqn. 36 to find

$$R(\text{semi-packed}) = \frac{1.29r_{3s}^2 - 4.29r_{3s} + 1}{\pi^2(r_{3s} - r_{3s}^2)} \qquad (44)$$

a relation which could also be obtained directly from eqn. 42 by setting $A = 0$.

To summarize the steps taken for calculating the porosity, the experimental quantities required are the slopes $b(\text{empty})$ and $b(\text{semi-packed})$, the lengths L_1 and L_2, the volumes $V_G'(\text{empty})$ and V_G and the value of γ from the previous determination. Using the values of $A(\text{empty}) = 4L_2^2/L_1^2$ and $R(\text{empty}) = V_G'(\text{empty})/V_G$ in the denominator of eqn. 26 or 36, its roots are found, the absolutely smallest one, $-r_3$ or $-r_2$, respectively, being retained. Then, using eqn. 41, $-r_{3s}$ is calculated. This is used, together with the new value of $A(\text{semi-packed}) = 4L_2^2/L_1^2\gamma$, in eqn. 42 or 44 to find $R(\text{semi-packed})$, and finally the latter and $R(\text{empty})$ are put in eqn. 43 to give ε.

In a previous paper[29] a much simpler relation (eqn. 4) was written for calculating ε, but that was only a first approximation, and a limiting case easily obtained from the more sophisticated equations derived here.

EXPERIMENTAL

Two chromatographs were used, equipped with devices for either flame ionization detection (FID) or thermal conductivity detection (TCD). In the first instance the lengths l' and l of the sampling cell (cf., Fig. 1) were each 103 cm and L_1 was 55 cm. In the second instance (with TCD), l' and l were each 72 cm and L_1 was 43.8–55.5 cm. The material of the above columns was either stainless steel or glass of I.D. 3.9–7.6 mm. The I.D. of vessel L_2 was 17.5 mm in all instances. The gas volumes V_G of columns L_1 ranged from 6.02 to 21.47 cm³, whereas V_G' of empty vessels L_2 was 7.90–14.95 cm³.

The carrier gas was nitrogen (FID) or helium (TCD) at flow-rates ranging from 0.333 to 0.500 cm³s⁻¹. The duration of the carrier gas flow reversal was 15 s.

The pressure drop along $l' + l$ was negligible, and the pressure inside the whole cell was 1 atm.

Six solid beds were used, two with glass beads of diameter 3 and 4 mm, one with pieces of marble of mesh size 120–150, one with γ-alumina of 10–22 mesh, a bed with

Chromosorb P of 60–80 mesh, and a bed with silica gel of 60–80 mesh. The solute gases were methane (FID) or nitrogen (TCD).

Before experiments were carried out with packed or semi-packed cells, the solid materials were conditioned *in situ* by heating them at 503 K for 20 h under a continuous flow of carrier gas. After conditioning, the oven gas was brought to the desired working temperature and kept there for 1 h. Then, 20 cm^3 of solute gas were injected, and after 24 h the actual experiments were performed by injecting 2 cm^3 of solute (methane or nitrogen), and repeatedly making 15-s flow reversals. The temperature of the thermal conductivity detector was always 373 K. Each experiment lasted about 2 h.

Plots and calculations were made with an RT-Unitron desk-top computer connected to a Star SG10 printer.

RESULTS AND DISCUSSION

Both the obstructive factors γ and the external porosities ε in the various solid beds were determined using four glass cells with different geometric characteristics, and therefore different A(empty) and R(empty) values. Table I gives all particulars of these cells, together with their A(empty) calculated according to eqn. 34, R(empty) found from eqn. 29 and the absolutely smallest root $-r_3$ of the denominator of eqn. 26.

In Table II obstructive factors and porosities measured with TCD are collected, and Table III gives the results of porosity measurements based on experiments with FID.

The calculations of γ values were made using eqn. 39, whereas for ε the procedure summarized in the paragraph following eqn. 44 was followed. The more precise eqns. 26 and 42 were employed in all ε calculations.

The obstructive factor for glass beads of diameter 3 mm was not very different when measured with a single tube L_1 of diameter 7.6 mm (cell No. 1) and with cell No. 2 having two vessels L_1 and L_2 of very different diameters (3.9 and 17.5 mm, respectively). The γ value found by Knox and McLaren[32] for glass beads of diameters 0.28 and 0.50 mm was 0.58–0.62, under very different experimental conditions and by a different method. With materials other than glass beads (alumina, Chromosorb P and silica gel) the γ values differed considerably from those of glass beads using identical experimental conditions. This is probably due to the irregularities in the shape of the particles.

As regards the porosity of the glass beads, when it was determined with nitrogen

TABLE I

CHARACTERISTICS OF THE FOUR CELLS USED TO DETERMINE THE OBSTRUCTIVE FACTOR AND THE POROSITY

Cell No.	L_1 (cm)	L_2 (cm)	V_G (cm^3)	V_G' (cm^3)	$10^2 A$(empty)	R(empty)	$-r_3$
1[a]	43.8	—	21.47	—	0	0	−0.2522
2	50.4	4.2	6.02	7.90	2.78	1.312	$-6.102 \cdot 10^{-2}$
3	55.0	6.0	9.59	14.95	4.76	1.559	$-5.313 \cdot 10^{-2}$
4	55.5	4.2	6.63	8.90	2.29	1.342	$-5.996 \cdot 10^{-2}$

[a] The I.D. of column L_1 in this cell was 7.6 mm, whereas in cells 2, 3 and 4 it was 3.9 mm.

TABLE II

OBSTRUCTIVE FACTORS γ AND EXTERNAL POROSITY ε OF SOLID BEDS, MEASURED WITH A THERMAL CONDUCTIVITY DETECTOR, HELIUM CARRIER GAS AND NITROGEN SOLUTE GAS

Cell No.	Packing material	Particle size	T (K)	γ	ε
1	Glass beads	Diameter 3 mm	323.2	0.757	—
2	Glass beads	Diameter 3 mm	323.2	0.862	0.498
4	Glass beads	Diameter 3 mm	313.2	—	0.495
2	γ-Alumina	10–22 mesh	323.2	0.331	0.997
2	Chromosorb P	60–80 mesh	323.2	0.643	0.858
2	Silica gel	60–80 mesh	323.2	0.195	0.863

as solute gas (Table II), it was found 0.498 and 0.495 at two temperatures. These values differ by only 4% from the calculated value of 0.478, cited for beds of spherical particles. The porosity with glass beds of smaller diameter (0.28 and 0.50 mm), found by Knox and McLaren[32] by the use of a different chromatographic method, was 0.38. However, with methane as solute gas (Table III), the glass beads of 4 mm diameter show a porosity that decreases with increasing temperature, which may be due to reversible adsorption of methane on the glass surface, the adsorption decreasing as the temperature rises. This is confirmed by the results obtained with γ-alumina (cf., Table III), where ε is greater than unity and decreases again with temperature rise. The apparent porosity in this instance is $\varepsilon(1 + k)$, k being the partition ratio of methane between the carrier gas and the solid surface. Dividing the apparent porosity in Table III by the calculated value of 0.478 for spherical particles, the value of $1 + k$ is obtained, and from this the k values in the last column in Table III are found. As expected, these values decrease with increasing temperature. This is not the first time that adsorption of methane on alumina has been detected. Non-zero partition ratios for methane have been determined previously[18]. These, together with the present results, stress the need to use a gaseous solute that is not sorbed by the solid material or does not interact with it in anyway. The porosity value of 0.997 for alumina, found

TABLE III

EXTERNAL POROSITY ε OF SOLID BEDS AND PARTITION RATIO k OF METHANE MEASURED WITH CELL NO. 3, USING A FLAME IONIZATION DETECTOR, NITROGEN CARRIER GAS AND METHANE SOLUTE GAS, AT VARIOUS TEMPERATURES

Packing material	Particle size	T (K)	ε	k
Glass beads	Diameter 4 mm	353.2	0.525	—
Glass beads	Diameter 4 mm	383.2	0.466	—
Glass beads	Diameter 4 mm	413.2	0.386	—
Marble pieces	120–150 mesh	322.2–423.2	0.455	—
γ-Alumina	10–22 mesh	353.2	1.321	1.764
γ-Alumina	10–22 mesh	383.2	1.156	1.418
γ-Alumina	10–22 mesh	413.2	0.875	0.831

with nitrogen as solute gas (Table II), is probably due to the contribution of the internal porosity of this material, which is highly porous.

The values of ε found for pieces of marble, Chromosorb P and silica gel appear to be normal.

REFERENCES

1 N. A. Katsanos and I. Georgiadou, *J. Chem. Soc., Chem. commun.*, (1980) 242.
2 N. A. Katsanos, *J. Chem. Soc., Faraday Trans. I*, 78 (1982) 1051.
3 G. Karaiskakis, N. A. Katsanos, I. Georgiadou and A. Lycourghiotis, *J. Chem. Soc., Faraday Trans. I*, 78 (1982) 2017.
4 M. Kotinopoulos, G. Karaiskakis and N. A. Katsanos, *J. Chem. Soc., Faraday Trans. I*, 78 (1982) 3379.
5 G. Karaiskakis, N. A. Katsanos and A. Lycourghiotis, *Can. J. Chem.*, 61 (1983) 1853.
6 N. A. Katsanos, G. Karaiskakis and A. Niotis, in *Proceedings of the 8th International Congress on Catalysis, West Berlin, 1984, Dechema*, Vol. III, Verlag Chemie, Weinheim, p. 143.
7 G. Karaiskakis and N. A. Katsanos, in *Proceedings of the 3rd Mediterranean Congress on Chemical Engineering, Barcelona, Spain*, 1984, p. 68.
8 N. A. Katsanos and M. Kotinopoulos, *J. Chem. Soc., Faraday Trans. I*, 81 (1985) 951.
9 N. A. Katsanos, G. Karaiskakis and A. Niotis, *J. Catal.*, 94 (1985) 376.
10 E. Dalas, N. A. Katsanos and G. Karaiskakis, *J. Chem. Soc., Faraday Trans. I*, 82 (1986) 2897.
11 B. V. Ioffe, N. A. Katsanos, L. A. Kokovina, A. N. Marinitsev and B. V. Stolyarov, *Kinet. Katal.*, 28 (1987) 805.
12 N. A. Katsanos, *Catal. Today*, 2 (1988) 605.
13 N. A. Katsanos and G. Karaiskakis, *J. Chromatogr.*, 237 (1982) 1.
14 N. A. Katsanos and G. Karaiskakis, *J. Chromatogr.*, 254 (1983) 15.
15 G. Karaiskakis, N. A. Katsanos and A. Niotis, *Chromatographia*, 17 (1983) 310.
16 G. Karaiskakis, A. Niotis and N. A. Katsanos, *J. Chromatogr. Sci.*, 22 (1984) 554.
17 G. Karaiskakis, *J. Chromatogr. Sci.*, 23 (1985) 360.
18 G. Karaiskakis, N. A. Katsanos and A. Niotis, *J. Chromatogr.*, 245 (1982) 21.
19 G. Karaiskakis, A. Lycourghiotis and N. A. Katsanos, *Chromatographia*, 15 (1982) 351.
20 G. Karaiskakis and N. A. Katsanos, *J. Phys. Chem.*, 88 (1984) 3674.
21 N. A. Katsanos, G. Karaiskakis and P. Agathonos, *J. Chromatogr.*, 349 (1986) 369.
22 N. A. Katsanos and G. Karaiskakis, *J. Chromatogr.*, 395 (1987) 423.
23 A. Niotis, N. A. Katsanos, G. Karaiskakis and M. Kotinopoulos, *Chromatographia*, 23 (1987) 447.
24 E. Dalas, G. Karaiskakis, N. A. Katsanos and A. Gounaris, *J. Chromatogr.*, 348 (1985) 339.
25 G. Karaiskakis, P. Agathonos, A. Niotis and N. A. Katsanos, *J. Chromatogr.*, 364 (1986) 79.
26 N. A. Katsanos and E. Dalas, *J. Phys. Chem.*, 91 (1987) 3103.
27 N. A. Katsanos, P. Agathonos and A. Niotis, *J. Phys. Chem.*, 92 (1988) 1645.
28 N. A. Katsanos and G. Karaiskakis, *Adv. Chromatogr.*, 24 (1984) 125.
29 N. A. Katsanos, *J. Chromatogr.*, 446 (1988) 39.
30 N. A. Katsanos and G. Karaiskakis, *Analyst (London)*, 112 (1987) 809.
31 N. A. Katsanos, *Flow Perturbation Gas Chromatography*, Marcel Dekker, New York, 1988.
32 J. H. Knox and L. McLaren, *Anal. Chem.*, 36 (1964) 1477.
33 F. Obberhettinger and L. Badii, *Tables of Laplace Transforms*, Springer, Berlin, 1973.
34 J. C. Giddings, *Anal. Chem.*, 35 (1963) 439.